

# High Step up DC-DC Converter with Closed Loop Control for PV Fed Induction Motor Drive Applications

MARRAPU SATYANARAYANA, JAMI DELEEP KUMAR

M.Tech Scholar, Assistant Professor

Department of Electrical & Electronics Engineering

Dadi Institute Of Engineering & Technology, Anakapalle, Visakhapatnam, A.P, India

**Abstract :** *Low voltage photo voltaic systems require highly efficient converters to deliver as much as possible energy to the load with high gain DC voltage conversion. This concept presents two efficient step-up DC/DC converters one composed of five identical phases driven interchangeably and latter partial parallel isolated converter with voltage doubler. Experimental validation of theoretical assumption and discussion on power losses has been carried out. The use of silicon carbide components and current sharing technique assures high efficiency within wide power range.*

**Key Words:** *DC-DC converter, High step-up, coupled inductor, ground leakage current, Induction motor drive.*

## I. INTRODUCTION

PV power systems are efficient alternate source to provide electrical energy. But the drawback with the PV system is high installation cost to decreases the installation cost we need to increase the efficiency of the PV system required the P.E interface. Most commonly boost converter is used but as gain of dc-dc converter increase its efficiency also increase. There are several converters are proposed in the literature to increase the voltage gain. Mainly dc- dc converters are classified into 2 types

1. Non – isolated dc-dc converters
2. Isolated dc-dc converters

The advantage of non-isolated dc- dc converters simple and low cost but disadvantage is its voltage gain is limited. The advantage of isolated dc-dc converter is high voltage gain but it has a disadvantage of high cost and more components. In the literature a hybrid boost converter is proposed to increase the voltage gain with simple structure [1], [2].

In many industries induction motor drive is used because of its low cost and low maintenance. Induction motors are design for high voltage to have high efficiency. By integrating the PV system we can reduce the energy consumption for integrating this PV system we are using a high voltage gain hybrid dc-dc converter and 3- level diode clamped inverter [3-6].

This work mainly focusing on integration of PV system with the induction motor using closed loop controlled hybrid dc-dc converter [7-10].

This paper explains the effective operation of Induction motor is based on the choice of suitable high voltage gain converter system that is fed to Induction Motor. Here the induction motor drive is control action is done with closed loop mode of system. The design and operation of proposed high voltage gain converter system that is fed to Induction Motor is simulated using MATLAB/SIMULINK.

## II. CIRCUIT CONFIGURATION AND ANALYSES

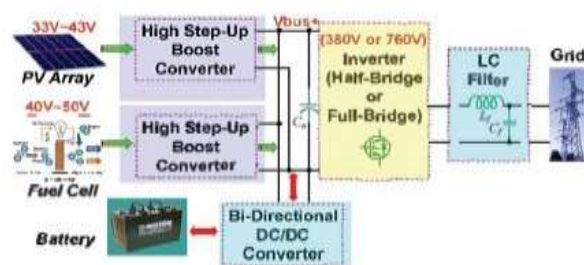


Fig.1. Diagram of a single-phase renewable energy grid-connected system

The improvements within renewable energy systems include improvements in energy conversion systems, such as PV arrays and fuel cells, and improvements in electrical circuits for managing the generated power. Fig.1 shows a hybrid renewable energy grid-connected system. The main challenges within designing these renewable systems are: efficient extracting electrical power from the energy conversion system and converting the generated power to the desired level and form. For instance, for the renewable energy system shown in Fig.3.1, the maximum possible generated power by the PV array must be extracted by the following power converter and then the low voltage of the PV module should be converted to a much higher voltage needed by the next block. Therefore, two important duties of the high step-up converters in Fig.1 are: Maximum Power Point Tracking (MPPT) and boosting the low generated voltage by PV array and fuel cell. So far, lots of researches are carried out to improve the efficiency, reliability, cost and life span of the DC-DC converters for renewable energy sources [1-10]. In [1-6] many DC-DC and DC-AC converters for this purpose are reviewed. For this application, conventional boost converter will be the first choice. But for the simple boost converter, the voltage stress of the switch and diode are equal to the high output voltage, where high-voltage rated components with high on-resistance should be used, which causes high

conduction losses. Moreover, in high duty cycles, high conduction losses and serious reverse recovery problems are caused. Hence, in the conversion ratios of more than 7 conventional boost converter is not a reasonable choice.

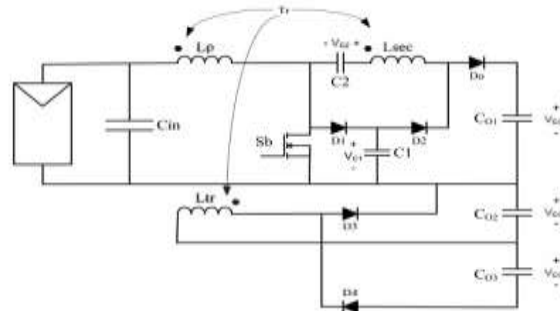


Fig.2. Proposed High Step-Up Converter.

The proposed DC-DC converter is depicted in Fig.2. This converter is a high step-up boost converter with coupled inductors. Switch  $S_b$  is the main switch.  $L_p$ ,  $L_{sec}$ , and  $L_{tr}$  represent individual inductors in the primary, secondary and tertiary sides of the coupled inductor ( $T_r$ ). Diodes  $D_1$  and  $D_2$  and capacitor  $C_1$  form the passive regenerative clamp circuit.  $C_2$  is a high voltage capacitor and is located in series with secondary side of the coupled inductor.  $D_3$ ,  $D_4$ ,  $C_{O1}$ ,  $C_{O2}$  and  $C_{O3}$  are output diodes and filter capacitors.

Primary and secondary sides of  $T_r$  along with capacitor  $C_2$  and snubber circuit form a high step-up boost converter and tertiary side of  $T_r$  along with diodes  $D_3$  and  $D_4$  form a combination of a DCM forward and a fly back converter.

In this section, the detailed operational modes of the DC-DC converter are described in section A, and then the converter is analyzed in section B. The key wave forms of the DC-DC converter and its operational modes are depicted in Fig.3 and Fig.4.

**A. OPERATIONAL MODES**

In order to simplify the circuit analysis, all electronic devices are considered ideal. The coupled inductor is modeled with an ideal transformer, a ( $L_{lk}$ ), and a magnetizing inductor ( $L_m$ ). Turns ratios and coupling coefficient are defined as:

$$n_1 = N_2 / N_1 \tag{1}$$

$$n_2 = N_3 / N_1 \tag{3.2}$$

$$k = L_m / (L_{lk} + L_m) \tag{3.3}$$

where  $N_1$ ,  $N_2$  and  $N_3$  are the winding turns of the primary, secondary, and tertiary sides of the coupled inductor.

**1) Mode 1 ( $t_0 - t_1$ ) [Fig.3 (a)]:**

When switch  $S_b$  is turned on, the magnetizing inductor is charging by the input voltage and its current is increasing linearly. Diode  $D_3$  is on and the tertiary current ( $i_{D3}$ ) is increasing because of the voltage difference between the capacitor  $C_{O2}$  and tertiary side which is established across the leakage inductor in tertiary side. Proportionally the current through secondary side is increasing. Hence, the secondary voltage in series with clamp voltage ( $V_{C1}$ ), charge the capacitor  $C_2$ .

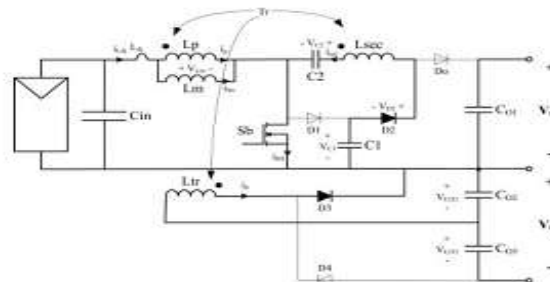


Fig.3 (a) mode 1

**2) Mode 2 ( $t_1 - t_2$ ) [Fig.3 (b)]:**

When switch  $S_b$  turns off, the leakage current along with secondary current charge the drain-source capacitor of the  $S_b$  and then diode  $D_1$  is turned on and the leakage and secondary currents start to charge the clamp capacitor  $C_1$ . Meanwhile, the current through leakage inductor decreases until equals to the current through magnetizing inductor, and then the current through primary, secondary and tertiary sides become zero.

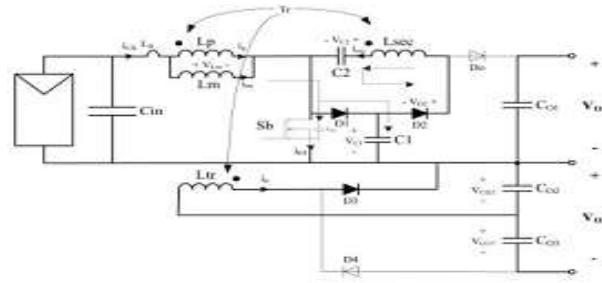


Fig.3 (b) mode 2

3) Mode 3 ( $t_2 - t_3$ ) [Fig.3 (c)]:

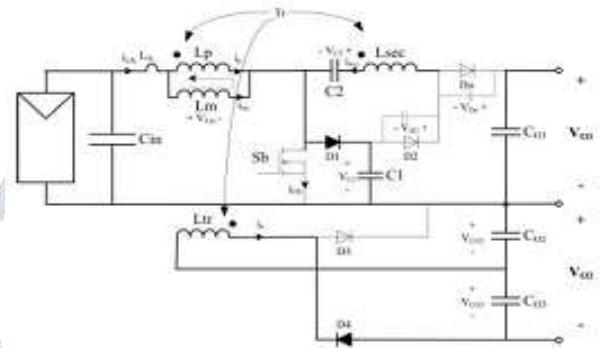


Fig.3 (c) mode 3

When leakage current becomes lower than magnetizing current, the direction of currents through transformer changes. At this moment, diode  $D_2$  is turned off and the voltage across diodes  $D_4$  and  $D_0$  are forced to decay to zero. Due to existence of leakage inductor, these diodes are switched under fully soft-switching condition.

4) Mode 4 ( $t_3 - t_4$ ) [Fig.3 (d)]:

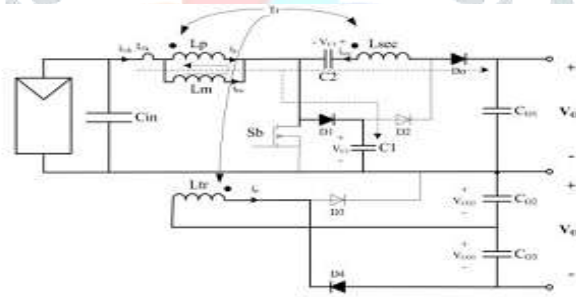


Fig.3 (d) mode 4

Once diode  $D_0$  turns on, the series voltages of input source, capacitor  $C_2$ , leakage inductor, magnetizing inductor and secondary side supply output capacitor  $C_{01}$ . Also, by conduction of  $D_4$ , the output capacitor  $C_{03}$  is charged by the current through tertiary side of transformer. Meanwhile, the leakage current is still charging the clamp capacitor  $C_1$ . During this mode, the clamp capacitor is charged, the diode  $D_1$  turns off and leakage current equals to the secondary current.

5) Mode 5 ( $t_4 - t_5$ ) [Fig.3 (e)]:

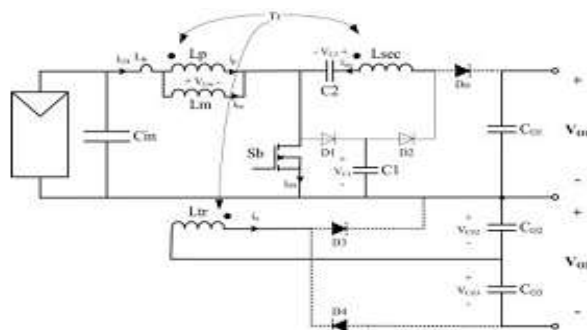


Fig.3 (e) mode 5

At the beginning of this mode, since the leakage current and the secondary current are equal, and also due to the limited raising rate of leakage current because of the leakage inductance, the switch  $S_b$  turns on under Zero current switching condition (ZCS). After  $S_b$  is turned on, the leakage inductor is charged until its current reaches the magnetizing current and then becomes greater. Meanwhile the

current through primary side of  $T_r$  becomes zero and then increases in the reverse direction. This change in the current through transformer causes the diodes  $D_0$  and  $D_4$  turn off and then the diodes  $D_3$  and  $D_2$  turn on.

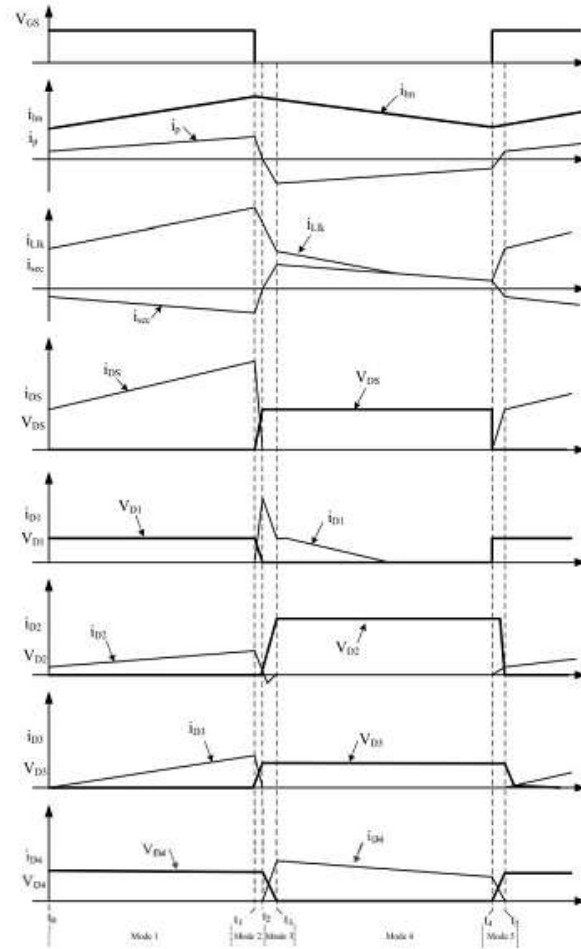


Fig.4. Key theoretical waveforms of the proposed converter.

**B. CONVERTER ANALYSIS**

In this part, the voltages of output capacitors are derived. To simplify the analysis, coupling coefficient of the transformer  $T_r$  is assumed unity. The magnetizing inductor of the transformer along with switch  $S_b$ , diode  $D_1$  and capacitor  $C_1$ , form a conventional boost converter and like any boost converter in CCM mode, the voltage of capacitor  $C_{p1}$  can be calculated as:

$$V_{C1} = \frac{V_m}{1 - D} \quad (4)$$

Where  $D$  is the duty cycle. The voltage across secondary side of the transformer is  $n_1$  times of the input voltage and the series voltages of secondary side and capacitor  $C_1$  charge the capacitor  $C_1$ . So the voltage across  $C_1$  can be calculated as:

$$V_{C2} = n_1 \cdot V_m + \frac{V_m}{1 - D} \quad (5)$$

When switch  $S_b$  turns off, the primary and secondary sides of the transformer along with capacitor  $C_2$  charge the capacitor  $C_{O1}$  and the following KVL is established:

$$V_{C_{O1}} = V_{in} - V_p + V_{C2} - V_{sec} \quad (6)$$

where  $V_p$  and  $V_{sec}$  are the voltages of the primary and secondary sides respectively. By (4), (5) and (6) the voltage of capacitor  $C_{O1}$  is derived as:

$$V_{C_{O1}} = \frac{2 + n_1}{1 - D} V_m \quad (7)$$

When switch  $S_b$  turns on, the capacitor  $C_{O2}$  is charged through the diode  $D_3$  and tertiary side of transformer. The difference voltage between tertiary side and the voltage of capacitor  $C_{O2}$  is located across the leakage inductor in tertiary side and forms a current that charges  $C_{O2}$  up to the tertiary voltage (assuming the coupling coefficient unity). Thus the voltage of capacitor  $C_{O2}$  can be calculated as:

$$V_{C_{O2}} = n_2 \cdot V_m \quad (8)$$



The capacitor  $C_{03}$  along with the tertiary side and the diode  $D_4$  form a fly back converter and when the switch  $S_b$  is off, the capacitor  $C_{03}$  is charge. Therefore, like any fly back converter in CCM mode, the voltage of capacitor  $C_m$  can be expressed as:

$$V_{C_{03}} = n_2 \cdot V_{in} \frac{D}{1-D} \quad (9)$$

The sum of capacitors  $C_{02}$  and  $C_{03}$  voltages form one of the converter outputs and can be expressed as:

$$V_{O2} = V_{C_{02}} + V_{C_{03}} = n_2 \cdot \frac{V_{in}}{1-D} \quad (10)$$

### III. DESIGN CONSIDERATION

If this converter is used for extracting power from a photovoltaic module, an MPPT algorithm must be used to control the converter. Since the proposed converter has a single-switch, implementation of MPPT algorithm is simple.

The difference voltage between capacitor  $C_{02}$  and the voltage of tertiary side, which is a relatively high voltage at the converter start up time, would be applied across the leakage inductor in the tertiary side and leads to a high current that can damage the main switch. Therefore, to avoid this high current at the starting, a soft-start must be considered for the control block.

If used for grid-connected applications, the output capacitors of the converter may have the roll of power decoupling capacitor. So, the minimum value of the output capacitors can be calculated as:

$$C = \frac{P}{2 \cdot \omega_{grid} \cdot V_c \cdot \Delta V_c} \quad (12)$$

where  $P$  is the nominal power of PV module,  $\omega_{grid}$  is the grid angular frequency,  $V_c$  is the mean voltage across the capacitor and  $\Delta V_c$  is the amplitude of voltage ripple [1].

By choosing a larger magnetizing inductor, the input current variations can be reduced and consequently a smaller input capacitor in parallel with the PV -module would be required. However, a large magnetizing inductor increases the volume, price and cost of the circuit.

A fast conductive device must be chosen as the clamp diode ( $D_1$ ) which its voltage stress is equal to the voltage stress of switch  $S_b$ . Schottky diodes are better choice for this purpose.

### IV. INDUCTION MOTOR

An asynchronous motor type of an induction motor is an AC electric motor in which the electric current in the rotor needed to produce torque is obtained by electromagnetic induction from the magnetic field of the stator winding. An induction motor can therefore be made without electrical connections to the rotor as are found in universal, DC and synchronous motors. An asynchronous motor's rotor can be either wound type or squirrel-cage type.

Three-phase squirrel-cage asynchronous motors are widely used in industrial drives because they are rugged, reliable and economical. Single-phase induction motors are used extensively for smaller loads, such as household appliances like fans. Although traditionally used in fixed-speed service, induction motors are increasingly being used with variable-frequency drives (VFDs) in variable-speed service. VFDs offer especially important energy savings opportunities for existing and prospective induction motors in variable-torque centrifugal fan, pump and compressor load applications. Squirrel cage induction motors are very widely used in both fixed-speed and variable-frequency drive (VFD) applications. Variable voltage and variable frequency drives are also used in variable-speed service.

In both induction and synchronous motors, the AC power supplied to the motor's stator creates a magnetic field that rotates in time with the AC oscillations. Whereas a synchronous motor's rotor turns at the same rate as the stator field, an induction motor's rotor rotates at a slower speed than the stator field. The induction motor stator's magnetic field is therefore changing or rotating relative to the rotor. This induces an opposing current in the induction motor's rotor, in effect the motor's secondary winding, when the latter is short-circuited or closed through external impedance. The rotating magnetic flux induces currents in the windings of the rotor; in a manner similar to currents induced in a transformer's secondary winding(s). The currents in the rotor windings in turn create magnetic fields in the rotor that react against the stator field. Due to Lenz's Law, the direction of the magnetic field created will be such as to oppose the change in current through the rotor windings. The cause of induced current in the rotor windings is the rotating stator magnetic field, so to oppose the change in rotor-winding currents the rotor will start to rotate in the direction of the rotating stator magnetic field. The rotor accelerates until the magnitude of induced rotor current and torque balances the applied load. Since rotation at synchronous speed would result in no induced rotor current, an induction motor always operates slower than synchronous speed. The difference, or "slip," between actual and synchronous speed varies from about 0.5 to 5.0% for standard Design B torque curve induction motors. The induction machine's essential character is that it is created solely by induction instead of being separately excited as in synchronous or DC machines or being self-magnetized as in permanent magnet motors.

For rotor currents to be induced the speed of the physical rotor must be lower than that of the stator's rotating magnetic field ( $n_s$ ); otherwise the magnetic field would not be moving relative to the rotor conductors and no currents would be induced. As the speed of the rotor drops below synchronous speed, the rotation rate of the magnetic field in the rotor increases, inducing more current in the windings and creating more torque. The ratio between the rotation rate of the magnetic field induced in the rotor and the rotation rate of the stator's rotating field is called slip. Under load, the speed drops and the slip increases enough to create sufficient torque to turn the load. For this reason, induction motors are sometimes referred to as asynchronous motors. An induction motor can be used as an induction generator, or it can be unrolled to form a linear induction motor which can directly generate linear motion.

#### Synchronous Speed:

The rotational speed of the rotating magnetic field is called as synchronous speed.

$$N_s = \frac{120 \times f}{P} \text{ (RPM)} \tag{13}$$

Where, f = frequency of the supply  
 P = number of poles

**Slip:**

Rotor tries to catch up the synchronous speed of the stator field, and hence it rotates. But in practice, rotor never succeeds in catching up. If rotor catches up the stator speed, there won't be any relative speed between the stator flux and the rotor, hence no induced rotor current and no torque production to maintain the rotation. However, this won't stop the motor, the rotor will slow down due to lost of torque, and the torque will again be exerted due to relative speed. That is why the rotor rotates at speed which is always less the synchronous speed.

The difference between the synchronous speed (Ns) and actual speed (N) of the rotor is called as slip.

$$\% \text{ slip } s = \frac{N_s - N}{N_s} \times 100 \tag{14}$$

**V. MATLAB/SIMULINK RESULTS**

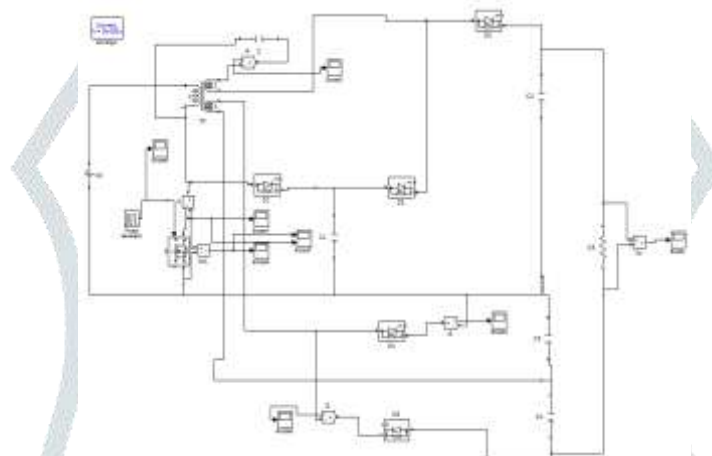
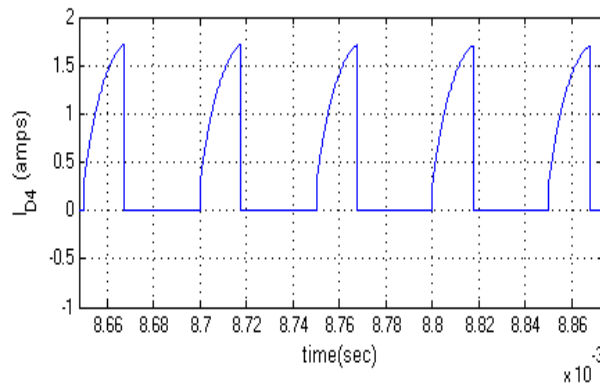
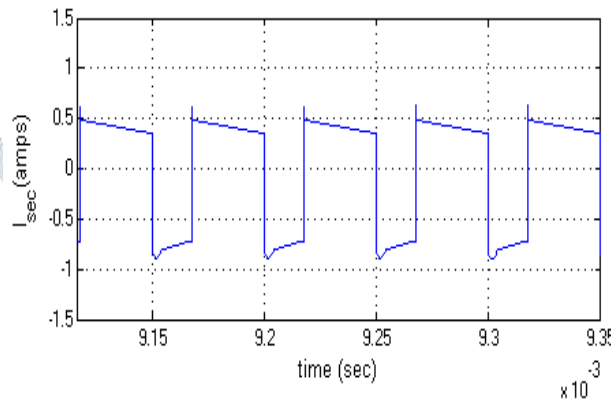


Fig.5 simulink model of step-up dc-dc converter



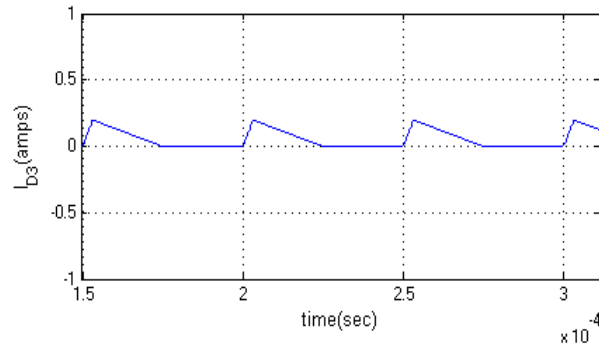


Fig.6 Current wave forms of the converter

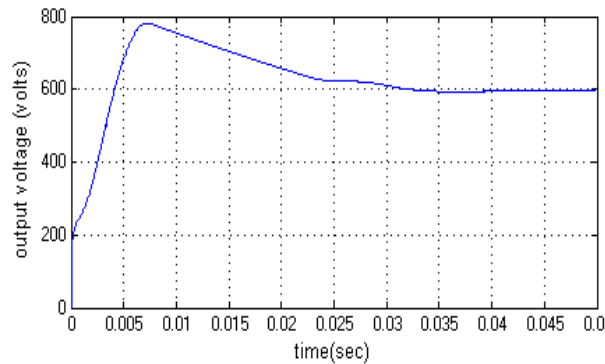


Fig.7 output voltage

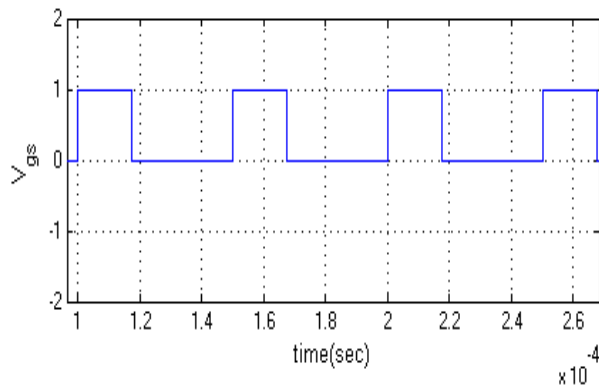


Fig.8 voltage ( $V_{gs}$ )

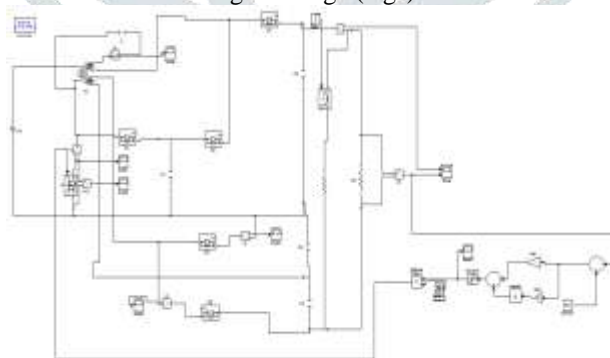


Fig.9 simulink model of step-up dc-dc converter with closed loop control

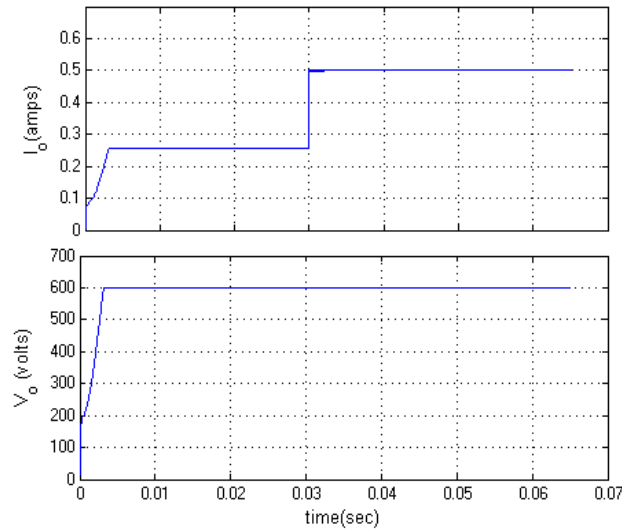


Fig.10 Voltage and Current wave forms with sudden increasing load

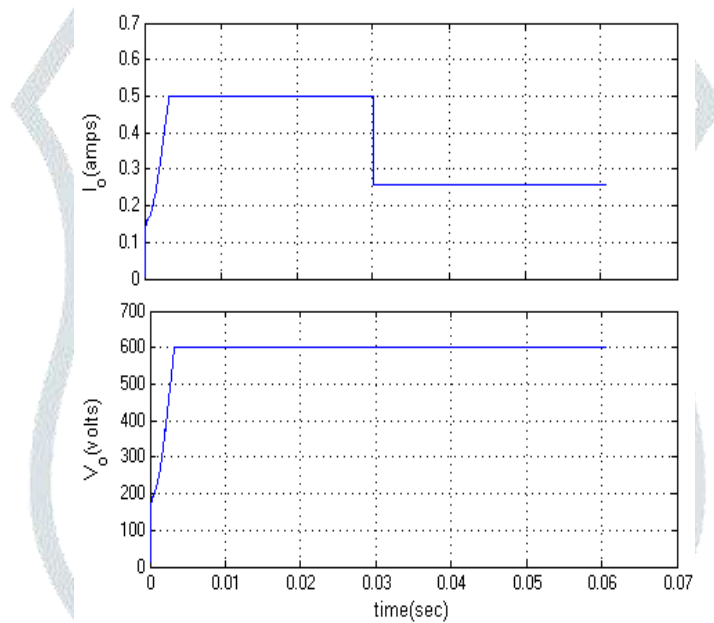


Fig.11 Voltage and Current wave forms with sudden decreasing load

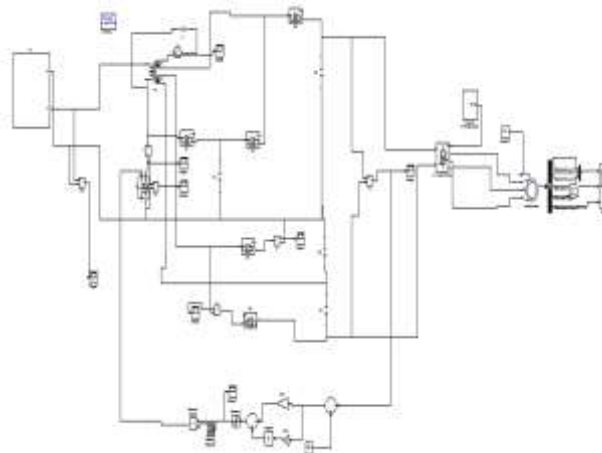


Fig.12 simulink model of PV system based step-up dc-dc converter with closed loop control for induction motor drive



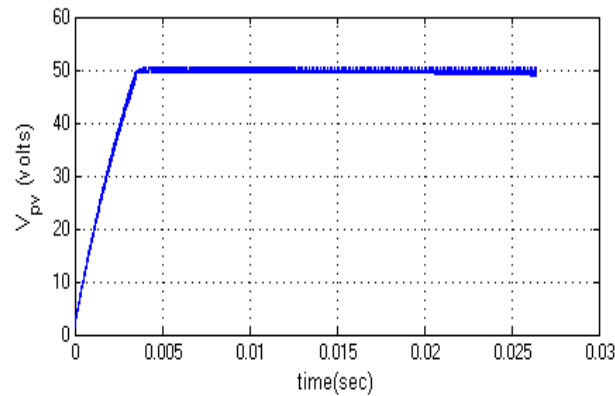


Fig.13 PV voltage

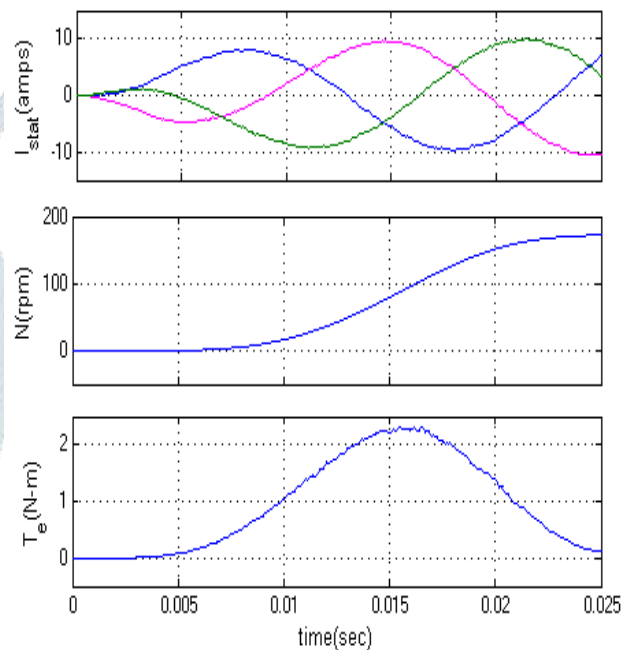


Fig.14 Stator current, Speed, Torque characteristics of the induction motor

## VI. CONCLUSION

This paper presents a solar PV system fed induction motor via MPPT based step-up DC-DC boost converter and an inverter which is controlled by closed loop technique. It is clear that this converter is very flexible to be used as a PV fed Dc power supply suitable for a single phase or three phase inverter as well as it can be used for a grid connected system. The advantage of this step-up DC-DC converter is simple, low cost and high efficiency. This paper has presented the simulation analysis of steady value related consideration, for the proposed converter operated under closed loop manner. The analysis of step-up DC-DC converter integrated with inverter feeding a three-phase induction motor drive is carried out and simulation results are presented.

## REFERENCES

- [1] S. M. Chen, T. J. Liang, L. S. Yang, and J. F. Chen, "A cascaded high stepup dc-dc converter with single switch for micro source applications," IEEE Trans. Power Electron., vol. 26, no. 4, pp. 1146–1153, Apr. 2011.
- [2] W. Li, X. Li, Y. Deng, J. Liu, and X. He, "A review of non-isolated high step-up dc/dc converters in renewable energy applications", 24th Annual Applied Power Electronics Conf. and Exposition (APEC) IEEE 1, pp: 364–369 year: 2009.
- [3] Neha Adhikari, Bhim Singh, A. L. Vyas, Ambrish Chandra Kamal-AIHaddad, "Analysis and Design of Isolated Solar-PV Energy Generating System", IEEE, year: 2011.
- [4] Mahajan Sagar Bhaskar Ranjana, Nandyala Sree ramula Reddy and Repalle Kusala Pavan Kumar" Non-Isolated Dual Output Hybrid DC-DC Multilevel Converter for Photovoltaic Applications", 2nd International Conference on Devices, Circuits and Systems (ICDCS),2014.
- [5] J. T. Bialasiewicz, "Renewable energy systems with photovoltaic power generators: Operation and modeling," IEEE Trans. Ind. Electron., vol. 55, no. 7, pp. 2752–2758, year: Jul. 2008
- [6] S. B. Kjaer, I. K. Pedersen, and F. Blaabjerg, "A review of single-phase grid-connected inverters for photovoltaic modules," IEEE Trans. ind. Electron., vol. 41, No. 5, Sep. 2005.
- [7] D. Meneses, F. Blaabjerg, O. Garc'ia, and I. A. Cobos, "Review and comparison of step-Up transformerless topologies for photovoltaic AC-module application," IEEE Trans. Power Electron., vol. 28, no. 6, pp. 2649-2663, June 2013.

- [8] Q. Li and P. Wolfs, "A Review of the Single Phase Photovoltaic Module Integrated Converter Topologies with Three Different DC Link Configurations," IEEE Trans. Power Electron., vol. 23, NO. 3, May 2008.
- [9] S. Y. Araujo, P. Zacharias, and R. Mallwitz, "Highly Efficient SinglePhase Transformerless Inverters for Grid-Connected Photovoltaic Systems," IEEE Trans. ind. Electron., vol. 57, no. 9, September 2010.
- [10] W. Li and X. He, "Review of Non isolated High-Step-Up DC/DC Converters in Photovoltaic Grid-Connected Applications," IEEE Trans. ind. Electron., vol. 58, no. 4, April 2011.

